THE ANALYSIS OF THREE ICING FLIGHTS WITH VARIOUS ICE ACCRETION STRUCTURES WHEN REACHING ICING DEGREE SEVERE

H.-E. Hoffmann

German Aerospace Research Establishment (DLR), Oberpfaffenhofen
Institute for Atmospheric Physics
Wessling / Obb., Federal Republic of Germany

Abstract

Three icing flights are discussed -one in the clouds of a high pressure area, the other both in the clouds of warmfronts- on which the aircraft related icing degree severe was reached. The ice accretion on the wing underside expanded to 50 and 70cm, far beyond the area which can be deiced pneumatically on the wing of the DLR icing research aircraft of Do 28 type. Other maximum ice accretion values were: Roughness 2 to 20mm, mass 90 to 180kg. The mean values of the cloudphysical parameters producing these maximum ice accretion values were: Total water content 0.16 to 0.22g/m^3 ; temperature -1.6 to -5.2 ^{o}C; median volume diameter 19 to 126 µm. The cloud pathes in the range of the warmfronts amounted only to 1/10 or 3/10 of the cloud path in the range of a high pressure area, for obtaining the maximum icing characteristics roughness and mass of the flight in the high pressure area. This can be explained by the larger particles, respectively by their greater collision efficiency, in the clouds of the warmfronts compared with those in the high pressure area.

Notations

Beg. I [km]	Beginning of icing of wing underside
Beg. P(c) [km]	Beginning of flight path in clouds
H [m]	Height above cloud base
Max. I [km]	Maximum of icing of wing underside
MVD [µm]	Median volume diameter determined by measurements of the PMS-instruments FSSP and OAP
P(c1) [km]	Flight path in clouds, example 1
P(c2) [km]	Flight path in clouds, example 2
P(c3) [km]	Flight path in clouds, example 3
T [^{o}C]	Static air temperature
t(c) [min]	Flight time in clouds
TWC(J.-W.) [g/m^3]	Total water content (water content from fluid and solid particles) measured by hot wire instrument Johnson-Williams
TWC(PMS) [g/m^3]	Total water content (water content from fluid and solid particles) measured by PMS-instruments FSSP and OAP

1. Introduction

On flights in icing clouds with the DLR icing research aircraft of Do 28 type (1,2), the connection is determined between the normalized and the aircraft related icing degree and cloudphysikal, cloud and meteorological synoptic parameters (3,4,5,6,7). The cloudphysical parameters influencing icing here are: Total water content (the water content from fluid and solid particles), particle size distribution, temperature and cloud phase. In this paper three icing flights are analyzed on which the aircraft related icing degree severe was obtained. Criterion for reaching the aircraft related icing degree was, because of wing icing, the Do 28 could not maintain its research velocity of 120 kt (≈ 220 km/h).
The steps of analysis of the three icing flights -in the following called example 1,2,3- in section 3 are: Photographs of the maximum iced wing underside; description of the meteorological synoptic situation; vertical structure of the cloudphysical parameters total water content, temperature, median volume diameter; particle size distribution of one point of each of the vertical structures; horizontal structure of the cloudphysical parameters total water content, temperature, median volume diameter; particle size distribution of one point of each of the horizontal structures; mean values of the cloudphysical parameters producing the maximum iced wing underside; informations on the ice accretion on the wing: Structure, maximum roughness, thickness on the front edge of the wing, extent on the wing underside.
In section 4, there are compared the different cloud pathes to reach the same icing characteristics. Points of reference for these comparisons are the maximum icing values of example 1.
This paper is an abstract of (8).

2. Measurement of the cloudphysical parameters and determining of wing icing.

The total water content on all particle diameters was measured using a Johnson–Williams hot wire instrument. The particle size distribution, represented by the median volume diameter, and the total water content as a function of particle diameter was determined by measurements of the PMS–instruments FSSP (particle diameter 0.5 to 47 µm) and OAP (particle diameter 20 to 600 µm). For measuring the static air temperature there was used a Rosemount platinum wire resistance thermometer, which is installed in a housing which can be deiced. Informations on wing icing were got by photographs and visually by one of the flight engineers(2).

3. Analysis of three icing flights with aircraft related icing degree severe

The three icing flights are called in the following example 1, example 2, example 3

3.1 Photographs of the maximum iced wing underside

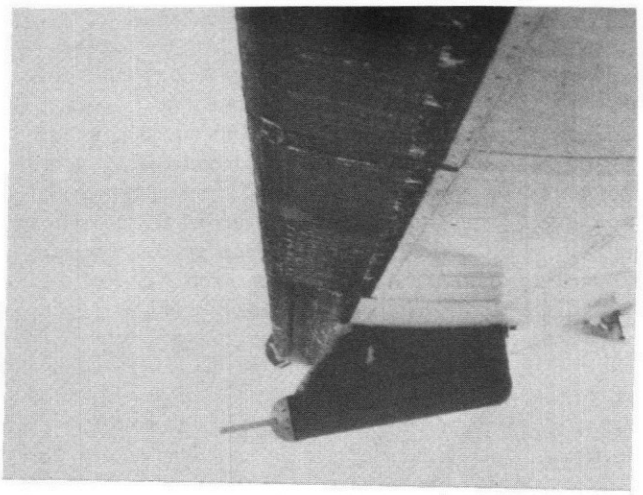

Fig. 1 The maximum iced wing underside, Example 1

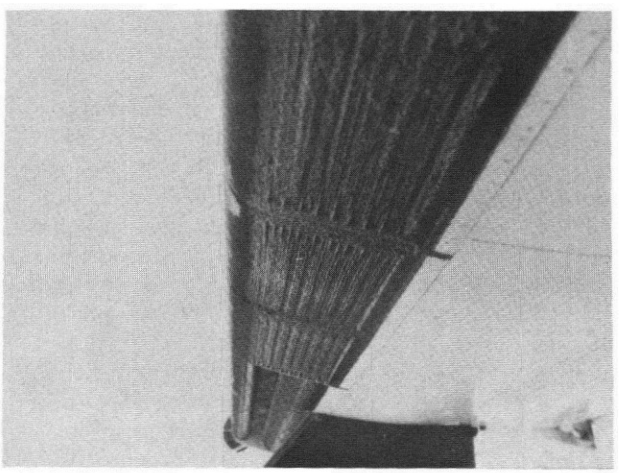

Fig. 2 The maximum iced wing underside, Example 2

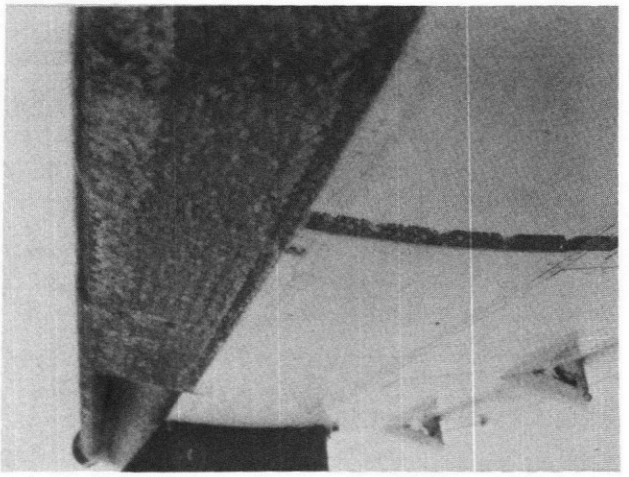

Fig. 3 The maximum iced wing underside, Example 3

In these three photographs, you can see the different structures of ice accretion and also, especially in the photographs of Fig. 1 and 3, that the extent of ice accretion was larger than the extent of the deicer boots. In the photographs, the black parts of the wing underside are the deicer boots.

3.2 Description of the meteorological synoptic situation

Example 1	In a high pressure area
Example 2	In the reach of a warmfront
Example 3	In the reach of a warmfront

Table 1. Meteorological synoptic situation

3.3 Vertikal structure of the cloudphysical parameters

In the following three Fig. 4,5,6 the cloudphysical parameters total water content, temperature and median volume diameter are plotted as a function of height above cloudbase for example 1,2,3. Each of the three figures represents the vertical structure of any point of the horizontal structures of the Fig. 9,10,11 (see section 3.5).

3.4 Particle size distribution of one point of the vertical structures of example 1,2,3 (see 3.3).

Here, in the Fig. 7 the total water content TWC (PMS) as a function of particle diameter D for one point of the vertical structures of examples 1,2,3 is shown. In the Fig. 8, for the same points of the vertical structures of examples 1,2,3, the total water content TWC (PMS) for the particle diameter ranges 2 to 32 µm, 33 to 310 µm and 311 to 600 µm is shown. Also here its part on the total water content of all the cloud particles in % is indicated. The points used, are representative for the whole vertical structure of the example 1,2,3.

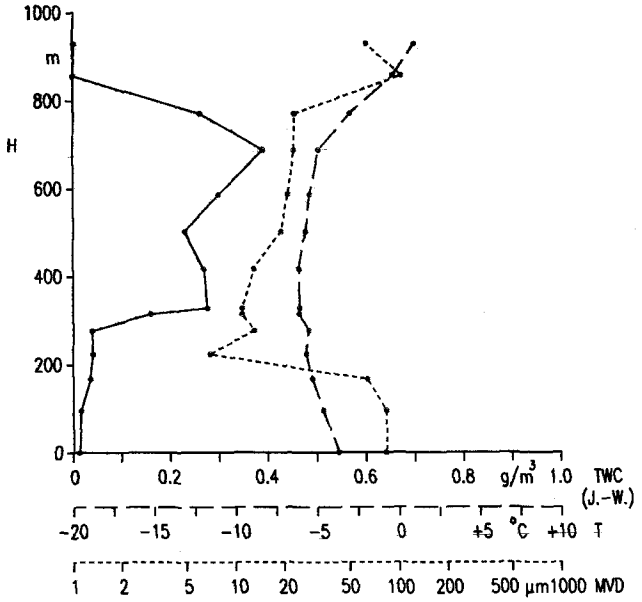

Fig. 4. Total water content TWC(J.–W.), temperature T and median volume diameter MVD as a function of height above cloudbase H.
Phase of particles: Fluid
Example 1

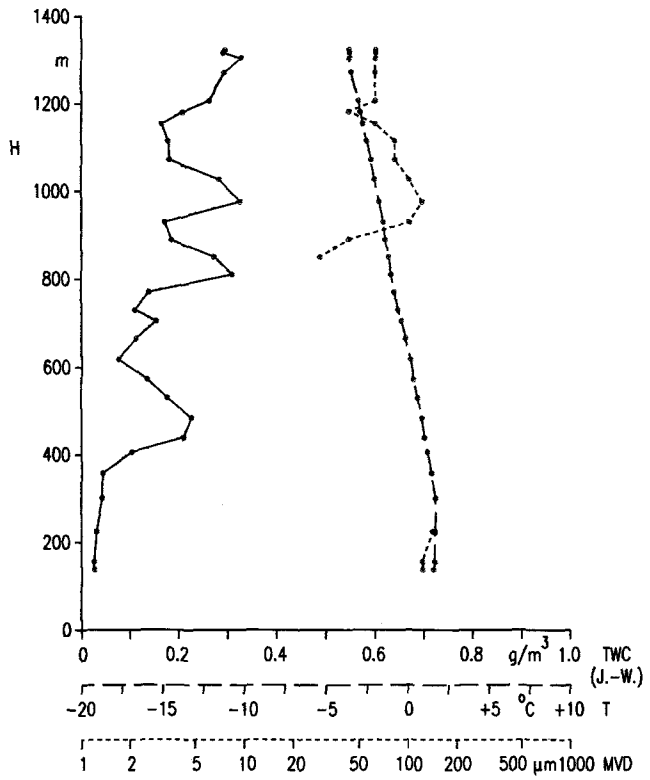

Fig. 6. Total water content TWC(J.–W.), temperature T, and median volume diameter MVD as a function of height above cloudbase H.
Phase of particles: Fluid
Example 3
(Between H 200 and 800m the measurements for MVD failed)

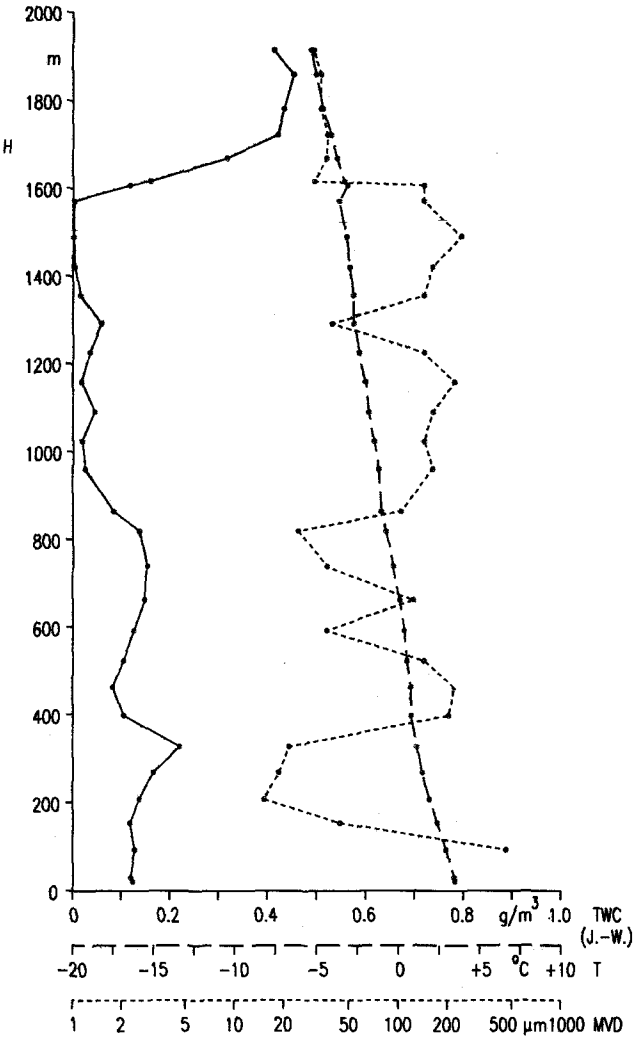

Fig. 5. Total water content TWC(J.–W.), temperature T, and median volume diameter MVD as a function of height above cloudbase H.
Phase of particles: Fluid/solid
Example 2

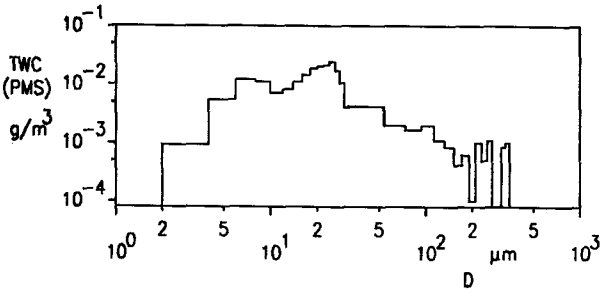

Example 1: Σ TWC(PMS): 0.20 g/m^3; MVD: 21 µm

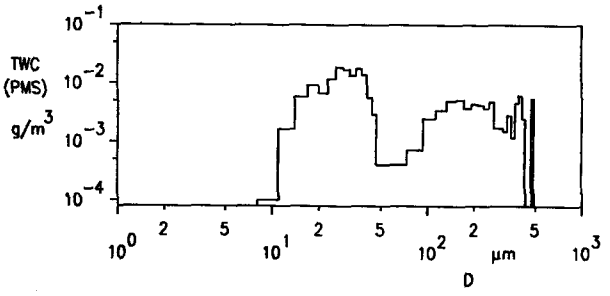

Example 2: Σ TWC(PMS): 0.14 g/m^3; MVD: 37 µm

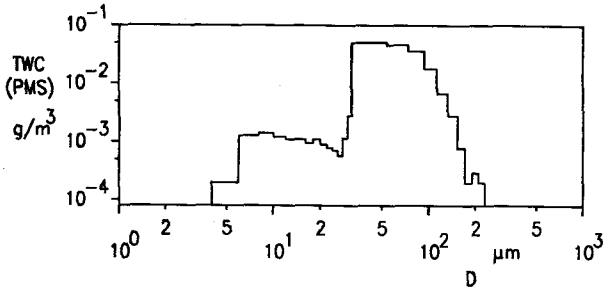

Example 3: Σ TWC(PMS): 0.18 g/m^3; MVD: 64 µm

Fig. 7. Total water content TWC(PMS) as a function of particle diameter D for one point of the vertical structures of example 1,2,3

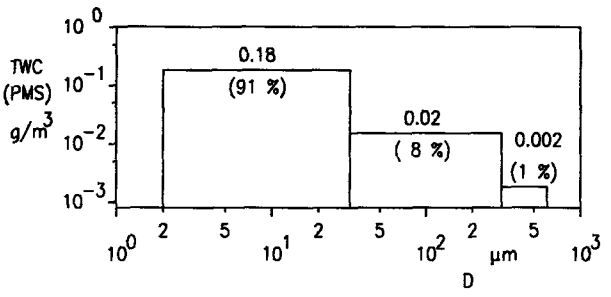

Example 1: Σ TWC(PMS): 0.20 g/m^3; MVD: 21 µm

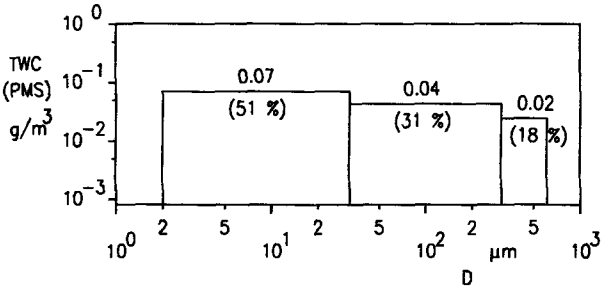

Example 2: Σ TWC(PMS): 0.14 g/m^3; MVD: 37 µm

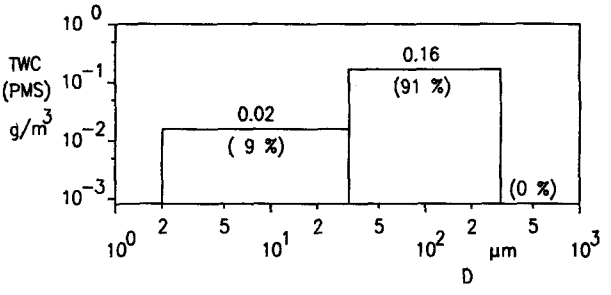

Example 3: Σ TWC(PMS): 0.18 g/m^3; MVD: 64 µm

Fig. 8. Total water content TWC(PMS) for the particle range 2 to 32 µm, 33 to 310 µm and 311 to 600 µm, and its part on the total water content of all the particles in % for one point of the vertical structure of example 1,2,3.

3.5 Horizontal structure of the cloudphysical parameters

In the following three Fig. 9,10,11, the values of the cloudphysical parameters total water content, temperature and median volume diameter are shown as a function of flight path respectively flight time in clouds.

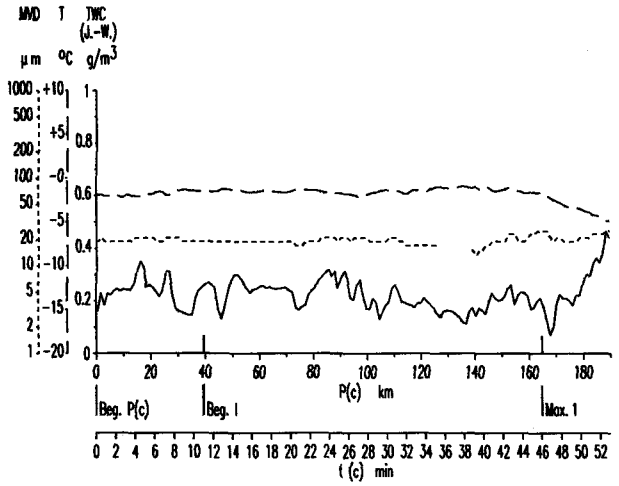

Fig. 9 Total water content TWC(J.–W.), temperature T, and median volume diameter MVD as a function of flight path in clouds P(c) respectively flight time in clouds t(c).
Beg.P(c): Beginning of flight path in clouds
Beg.I: Beginning of icing of wing underside
Max.I: Maximum of icing of wing underside (see Fig. 1)
Example 1

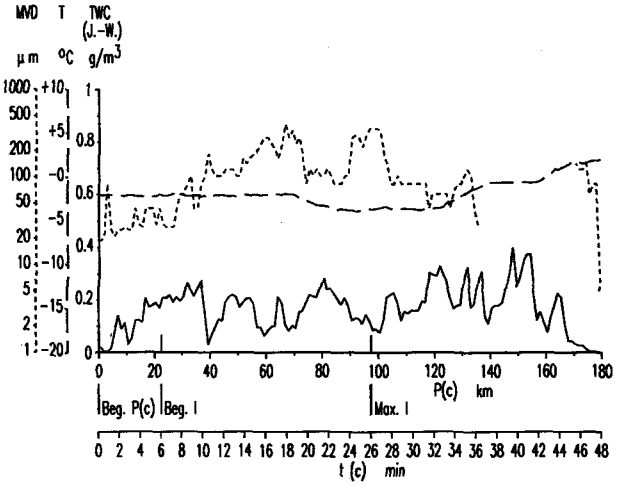

Fig. 11 Total water content TWC(J.–W.), temperature T, and median volume diameter MVD as a function of flight path in clouds P(c) respectively flight time in clouds t(c).
Beg.P(c): Beginning of flight path in clouds
Beg.I: Beginning of icing of wing underside
Max.I: Maximum of icing of wing underside (see Fig. 3)
Example 3

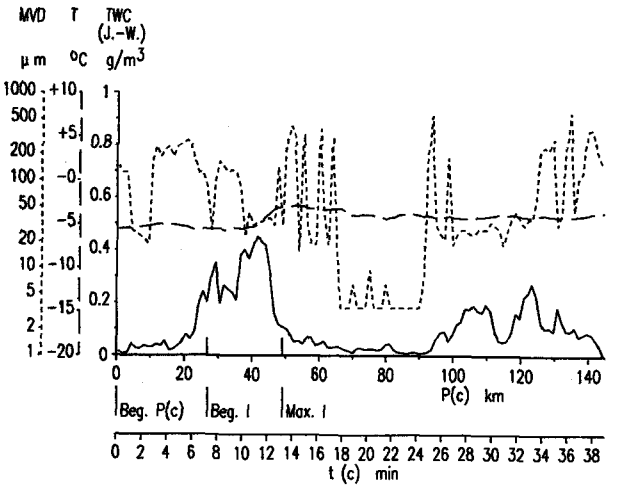

Fig. 10 Total water content TWC(J.–W.), temperature T, and median volume diameter MVD as a function of flight path in clouds P(c) respectively flight time in clouds t(c).
Beg.P(c): Beginning of flight path in clouds
Beg.I: Beginning of icing of wing underside
Max.I: Maximum of icing of wing underside (see Fig. 2)
Example 2

3.6 Particle size distribution of one point of the horizontal structures of examples 1,2,3 (see 3.5).

In the Fig. 12 the total water content TWC (PMS) as a function of particle diameter D for one point of the horizontal structures of examples 1,2,3 is shown. In the Fig. 13, for the same points of the horizontal structures of examples 1,2,3, the total water content TWC (PMS) for the particle diameter ranges 2 to 32 µm, 33 to 310 µm and 311 to 600 µm is shown. Also here its part on the total water content of all the cloud particles in % is indicated. The points used, are representative for the whole horizontal structure of examples 1,2,3.

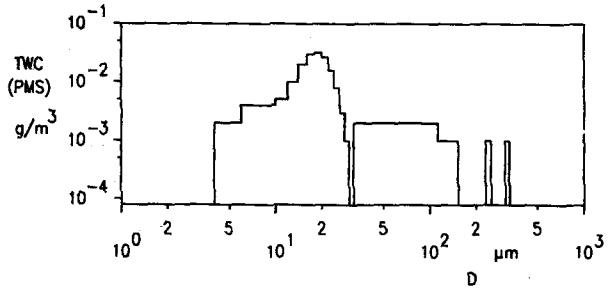

Example 1: Σ TWC(PMS): 0.17 g/m^3; MVD: 19 µm

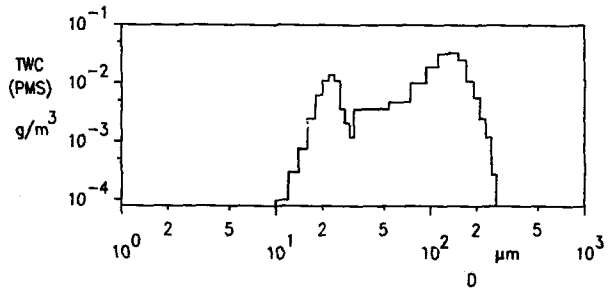

Example 2: Σ TWC(PMS): 0.21 g/m^3; MVD:123 µm

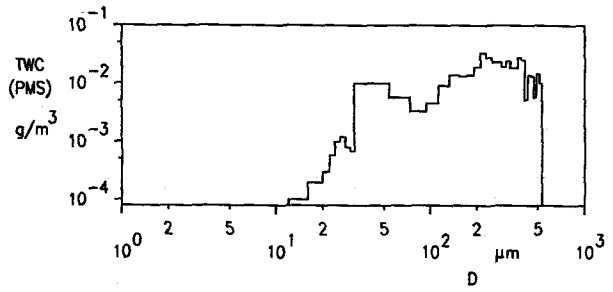

Example 3: Σ TWC(PMS): 0.41 g/m^3; MVD:281 µm

Fig. 12. Total water content TWC(PMS) as a function of particle diameter D for one point of the horizontal structures of example 1,2,3

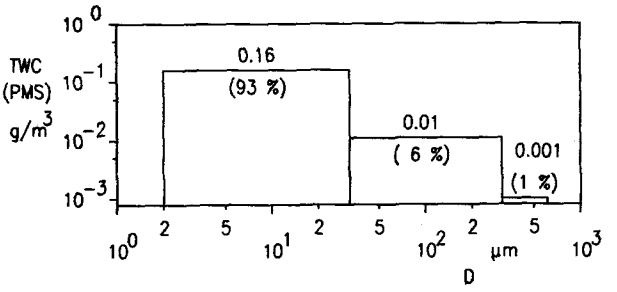

Example 1: Σ TWC(PMS): 0.17 g/m^3; MVD: 19 µm

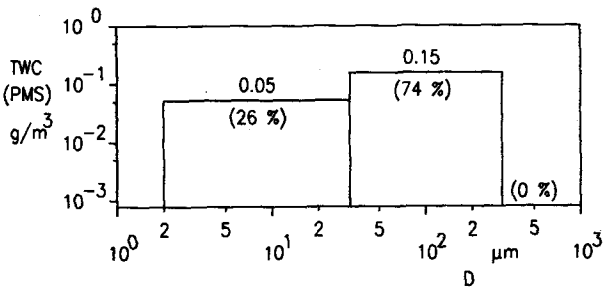

Example 2: Σ TWC(PMS): 0.21 g/m^3; MVD:123 µm

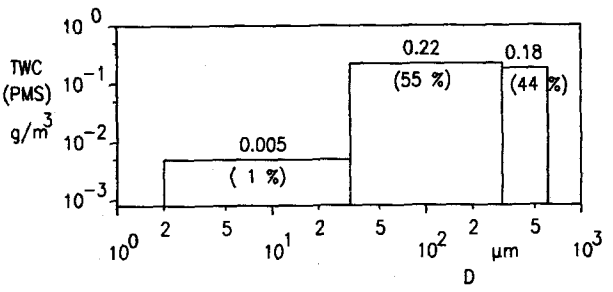

Example 3: Σ TWC(PMS): 0.41 g/m^3; MVD:281 µm

Fig. 13. Total water content TWC(PMS) for the particle ranges 2 to 32 µm, 33 to 310 µm and 311 to 600 µm, and its part on the total water content of all the particles in % for one point of the horizontal structures of example 1,2,3.

3.7 Mean values of the cloudphysical parameters producing the maximum iced wing underside (see 1,2,3).

	$\overline{TWC}$ (J.-W.) [g/m^3]	$\overline{T}$ [°C]	$\overline{MVD}$ [µm]
Example 1	0.22	−1.6	19
Example 2	0.17	−5.2	117
Example 3	0.16	−2.5	126

Table 2. Mean values of the cloudphysical parameters producing the maximum iced wing underside

3.8 Informations on the ice accretion on the wing: Structure, maximum roughness, maximum mass, maximum extent on the wing underside; thickness on the front edge, extent on the wing underside as a function of time

For calculating the ice mass, a density value of 0.91g/m^3 was taken.

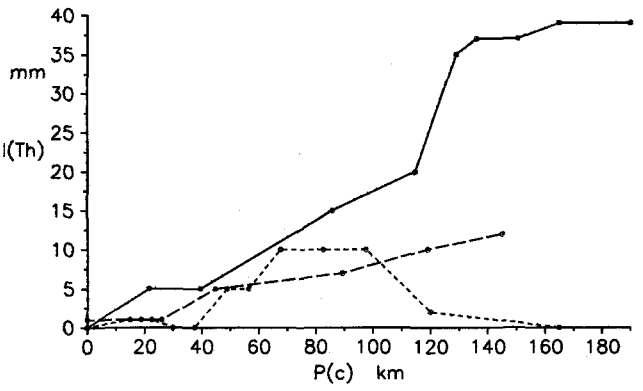

Fig. 14. Thickness of ice accretion on the front edge of the wing I(Th) as a function of flight path in clouds P(c) for the example 1,2,3
Example 1: ——; Example 2: – – – –; Example 3: ·····

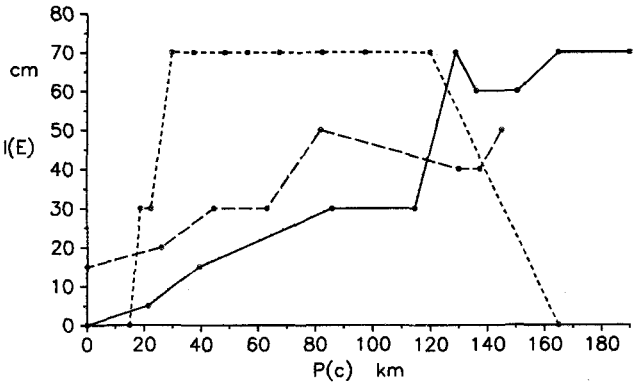

Fig. 15. Extent of ice accretion on the wing underside I(E) as a funtion of flight path in clouds P(c) for the example 1,2,3
Example 1: ——; Example 2: – – – –; Example 3: ·····

	Structure on the wing underside	Max. roughness on the wing underside [mm]	Max. mass on the wing underside [kg]	Max. extent on the wing underside [cm]	Max. thickness on the front edge [mm]
Example 1	Parallel to the direction of air flow	∿2	∿90	∿70	∿40
Example 2	Vertical to the direction of air flow	∿10	∿96	∿50	∿12
Example 3	Irregular	∿20	∿180	∿70	∿10

Table 3. Informations on the ice accretion on the wing

4. Comparison of the flight pathes in clouds of the examples 1,2,3 for reaching the same values of ice accretion criterions roughness and mass

In the following the flight pathes in clouds of examples 1,2,3 are compared for obtaining the same values of ice accretion criterions roughness and mass. Reference quantity are the maximum values of example 1. If P(c)1 max is the flight path in clouds to reach the maximum value in example 1, then P(c)2 respectively P(c)3 are the flight pathes in clouds to reach the same value in example 2 and example 3.
For calculating P(c)2 and P(c)3 it was assumed that the growth of ice accretion between beginning of icing of wing underside and maximum of icing of wing underside (s. Beg.I and Max.I in Fig. 10 and 11) was linear.

Concerning ice roughness on the wing underside

P(c)1max	P(c)2	P(c)3
=165km	: 32km	: 13km
= 1	: ∿0.2	: ∿0.1

Concerning ice mass on the wing underside

P(c)1max	P(c)2	P(c)3
=165km	: 45km	: 49km
= 1	: ∿0.3	: ∿0.3

Table 4. Flight pathes in clouds for obtaining the same values of ice accretion criterions roughness and mass

5. Conclusions

1. On the three icing flights discussed here, on which the aircraft related icing degree severe was reached, the following maximum ice accretion values on the wing were obtained: Roughness on the wing underside: 2 to 20mm; mass: 90 to 180kg; extent on the wing underside: 50 to 70cm; thickness on the front edge: 10 to 40mm.

2. The extent of the ice accretion on the wing underside was between 20 and 30cm larger than the extent of the boots for deicing. (The extent of the boots for deicing of aircraft Do 28 type is 30cm).

3. The flight path in clouds to obtain the same ice accretion values was depending on type of clouds. In the clouds of the warmfronts, the flight path in clouds was much shorter than that in clouds of a high pressure area for obtaining equal ice accretion values. To obtain the maximum ice accretion values for roughness and mass of the flight in the high pressure area, in the clouds of the warmfront only

of the flight path in clouds in the high pressure area was needed.

4. The main differences between the cloudphysical parameters of the clouds of a high pressure area (example 1) and the cloudphysical parameters of the clouds of a warmfront were those of the median volume diameters. In the clouds of the high pressure area there were predominantly small cloud particles and in the clouds of the warmfronts there were predominantly large cloud particles.

5. By the different sizes of the cloud particles, the different flight pathes in clouds to obtain the same ice accretion value can be explained: The larger the size of the cloud particles the greater their collision efficiency (3.9).

References

(1) Hoffmann, H.-E.; Demmel, J.: First Stage of Equipping a Type Do 28 as a Research Aircraft for Icing, and First Research Results. ESA-TT-855, 1984.

(2) Hoffmann, H.-E.; Demmel, J.: DFVLR's Research Aircraft Do 28, D-IFMP, and its Measuring Equipment. ESA-TT-972, 1986.

(3) Forcasters Guide on Aircraft Icing. Air Weather Service, AWS/TR-80/001, 1980.

(4) Hoffmann, H.-E.; Roth, R.; Demmel, J.: Standardized Ice Accretion Thickness as a Function of Cloud Physics Parameters, ESA-TT-1080, 1987.

(5) Hoffmann, H.-E.: Icing Degree Moderate to Severe: If and Where in Clouds. ICAS Proceedings, Jerusalem August 28 - September 2, 1988.

(6) Hoffmann, H.-E.: The Horizontal and Vertical Structures of Cloud Physical Parameters. WMP Report No. 12, WMO Scientific Conference on Weather Modification and Applied Cloud Physics, Beijing, China 8-12 May, 1989.

(7) Hoffmann, H.-E.; Roth, R.: Cloudphysical Parameters in Dependence on Height above Cloud Base in Different Clouds. Meteorology and Atmospheric Physics, 41,247-254, 1989.

(8) Hoffmann, H.-E.; Demmel, J.: An Analysis of three Icing Flights with Reaching the Aircraft Related Icing Degree Severe. DLR-Report. (In preparation).

(9) Jones, R. F.: Ice Formation on Aircraft. WMO-No. 109, TP-47, 1961.